ON STREAM SOLUTION OF A PROTOTYPE 8000 HP MOTOR INSTABILITY PROBLEM

by

Perry C. Monroe, Jr.

Staff Engineer, Machinery

Exxon Chemical Americas

Baytown, Texas

and

Dana J. Salamone

Chief Engineer

Centritech Corporation

Houston, Texas

Perry C. Monroe, Jr. is a staff engineer in the Mechanical Technical Service Section at the Exxon Chemical Americas Baytown, Texas plant. In this position, he provides technical support to maintenance and process activities, and he conducts training on turbomachinery-related subjects. Prior to joining Exxon, he spent eighteen months in East Kalimantan, Indonesia (Borneo) with Roy M. Huffington, Inc. at the P. T. Badak LNG Plant, as Assistant Maintenance Manager and Logistics Manager.

Mr. Monroe graduated from Auburn University in 1966 with a B.S. Degree in Mechanical Engineering, and he has worked for the past seventeen years in the areas of turbomachinery repair techniques, optical and mechanical alignment, vibration analysis and field balancing, non-destruction testing, mechanical seals, and corrosion. Prior to graduation, he worked as a designer of rocket engine components for NASA at Redstone Arsenal in Huntsville, Alabama, and as a draftsman for T.C.I. (U.S.S.) Steel Works in Birmingham, Alabama.

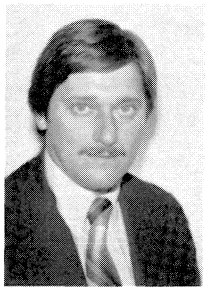

Dana J. Salamone is Chief Engineer for Centritech Corporation in Houston, Texas. In this capacity, he is a bearing designer and consultant to the utility, petroleum and chemical industries for the solution of turbomachinery vibration problems. He has nine years of industrial experience in stress analysis, structural vibrations, and rotor dynamics. Mr. Salamone earned his B.S. degree in Mechanical Engineering in 1974, and his M.S. degree in Applied Mechanics in 1977, both from the University of Virginia. He is a member of ASME and has authored several ASME publications in the area of rotor dynamics. He is also a registered professional engineer in the State of Texas.

ABSTRACT

This paper presents a typical field problem that most maintenance engineers in any petrochemical plant could encounter. Two 4000 hp through-drive electric motors were totally destroyed when the inboard coupling failed. Market conditions dictated that the compressor be put back into service as expeditiously as possible. A 3600 rpm prototype 8000 hp motor which could be fitted on the existing foundation was acquired from a power company. The existing half shell journal bearings had to be converted to a full shell design in order to solve a vibration problem. After start-up, the motor was plagued with a random vibration problem which occurred during a load change. Vibration data taken during one of these excursions indicated sub-synchronous frequencies at half-speed, which were equal in amplitude to the horizontal readings at synchronous speed. A computer model simulating the rotor and bearing systems indicated a whirl instability problem at 1800 rpm. The computer was used to design and optimize a "between the pad," four shoe tilting pad bearing which was installed during the December 1982 turnaround. The paper goes into details on the new bearing design and installation, motor mechanical and hot optical alignment, and start-up data.

All of the design and fabrication of the bearings was done while the unit was running, and the bearings were installed during a normal scheduled downtime. The result was a "first try fix." This example illustrates that the "trial and error" method of problem solving should be done on paper and not with hardware, particularly when the stakes are high and the time short. Equipment and techniques used to solve this problem are well established and used daily in most petrochemical plants.

INTRODUCTION

The compressor train in question was a five stage rotor with a 112 inch case that operated at 3600 rpm. A pair of tandem mounted (through-drive) 4000 hp, 2300 volt induction motors was connected to the compressor via continuously lubricated marine type gear couplings. This ammonia circulation compressor was installed as original equipment in 1964 and had given good service.

The motors were cleaned, and one coupling was replaced during a scheduled turnaround in the first quarter of 1980. During this time, X-Y non-contact probes were installed in the compressor and motor bearings. This vibration monitoring system had not been completed at the time of the catastrophic wreck.

On December 17, 1981, while operating in a normal, stabilized mode and without prior noticeable warning, the motor-to-compressor coupling apparently failed. This failure resulted in the breaking of two couplings, one motor shaft, and three motor bearings, with rotor and winding damage to both motors.

In order to meet product delivery schedules, the com-

pressor drivers had to be repaired promptly. The two alternatives were to repair the extensively damaged 4000 hp motors or to install a new motor (or motors). A decision was made to purchase a new 8000 hp prototype induction motor from a power company. Driver requirements were as follows:

- 8000 hp at 3600 rpm.
- Mountable on existing baseplate with minor modifications.
- Available for installation prior to product shipment deadline.

BACKGROUND

The ammonia circulation compressor had been operating continuously since 1980, except for a two week period, at approximately 92% of full load. Prior to the wreck (20-30 minutes), operating technicians had been on the compressor deck and had observed no abnormalities. Both operators were in the unit control room during the wreck and heard an abnormal grinding and surging sound. Within 15 seconds of the failure, the operators had reached the compressor deck in time to observe that the motors had stopped rotating but that the compressor had not. Due to excessive bearing housing damage, three lube oil pumps were running and spraying oil 30-40 feet into the air. The compressor-to-motor coupling guard was torn away, and a 2½ foot piece of the inboard motor shaft was lying on the compressor deck beside the motor. Both the inboard motor cast iron bearing housings and the coupling end housing of the outboard motor were shattered. See Figures 1 through 9 for details of damage.

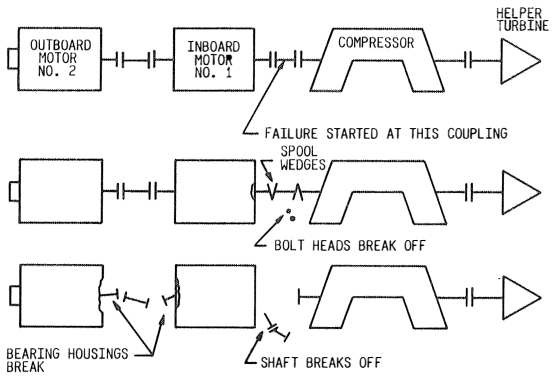

Figure 1. Ammonia Circulation Compressor Train. 8000 hp/3600 rpm.

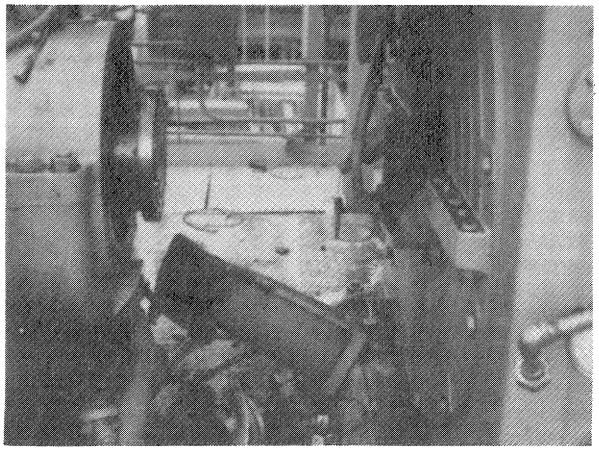

Figure 2. Compressor on Left and Inboard Motor at Right. Note Half of Coupling Guard and Damaged Oil Piping.

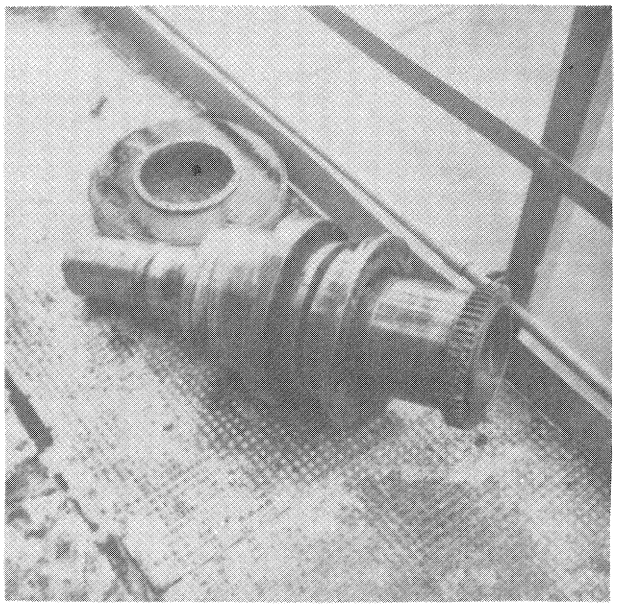

Figure 3. Inboard Motor Shaft and Coupling.

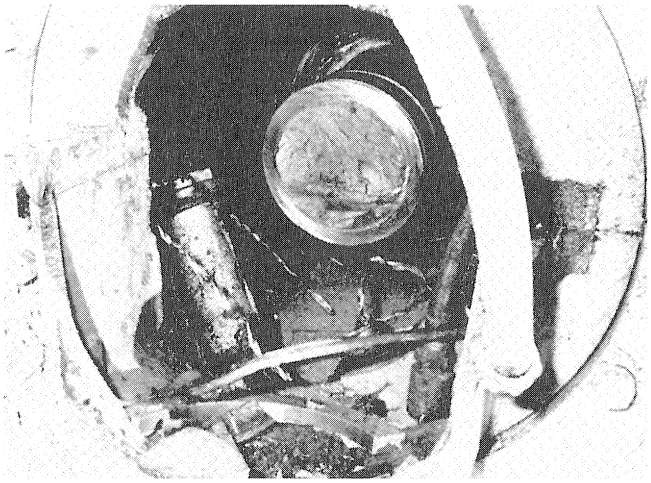

Figure 4. Looking Through Damaged Bearing Housing of Inboard Motor at Broken Shaft End.

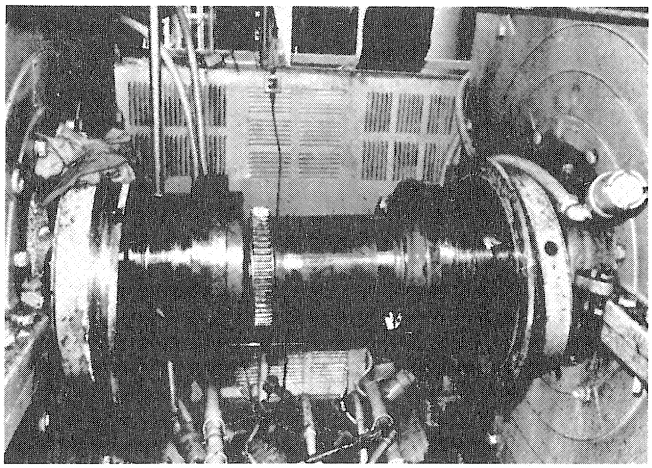

Figure 5. Condition of Coupling Between the Two Motors After Removal of Guard.

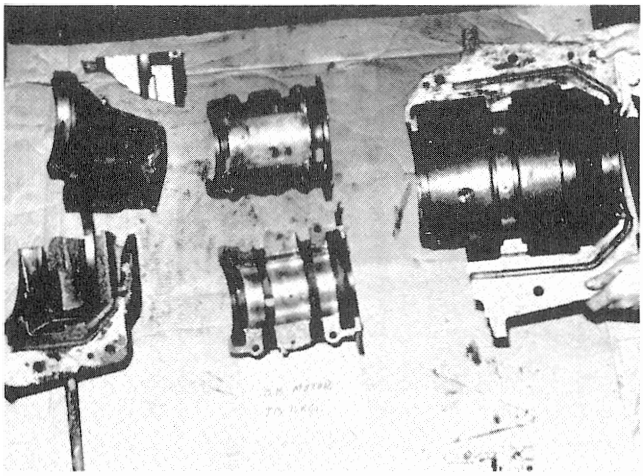

Figure 6. Part of Lower Bearing Housing at Left and Upper Housing at Right. Note Minimum Babbitt Damage from Radial Loads, but Severe Axial Shear Damage to the Bearing Shoulder.

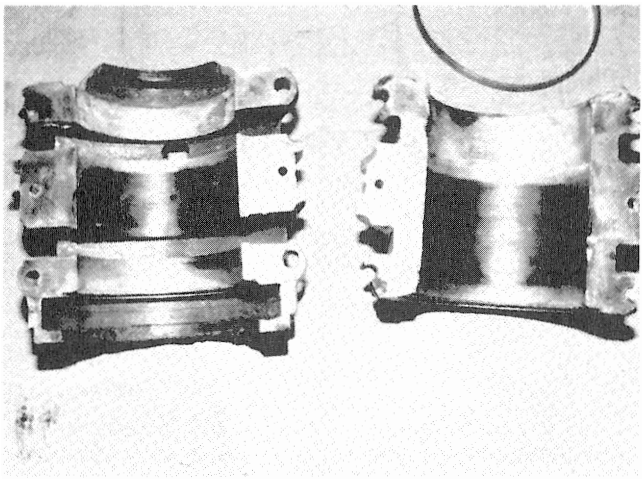

Figure 7. Outboard Bearing of Inboard Motor—Top Half on Left. Note that all Babbitt Damage from Radial Loads, but Severe Axial Shear Damage to the Bearing Shoulder.

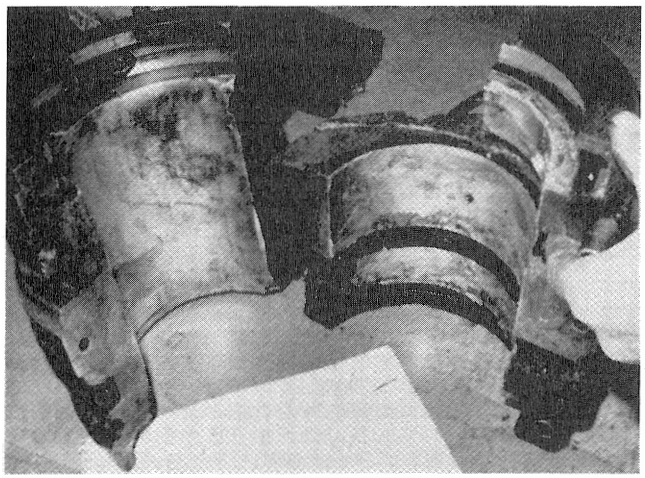

Figure 8. Inboard Bearing of Inboard Motor. Note Only Impact Type Damage to Babbitt and Shell.

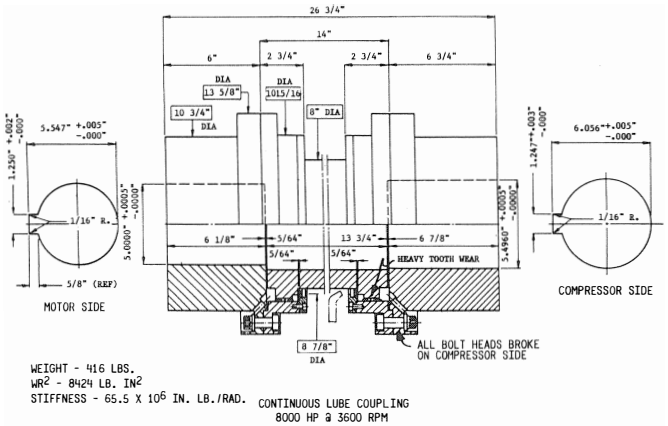

Figure 9. Continuous Lube Coupling. 8000 hp/3600 rpm.

Figure 9 illustrates the heavy tooth wear on the compressor side coupling shroud and hub, as well as the bolt head failures. Because of the extensive damage, reconstruction of the initial failure point was impossible. However, after talking to the coupling manufacturer, it was felt that a failure of the compressor-motor coupling was the cause of damage to the outboard bearing of the inboard motor. This led to the coupling bolt head breakage, which caused the coupling spacer to rotate off center and out of balance with the motor. The rotating wedge action of the coupling spool between the motor and compressor shafts produced a heavy axial impact load that fractured the motor bearing housings. Rotor and stator damage to the inboard motor caused a phase-to-ground short, which shut the compressor train down.

Examination of the compressor train files revealed a history of rapid gear tooth wear on the compressor-motor coupling. In 1978 the coupling specification was changed to incorporate nitrided gear teeth, in order to reduce this tendency. A nitrided coupling was not available during the 1980 downtime, so standard couplings were installed. Excessive gear tooth deterioration was very likely after twenty months of operation.

Continuous vibration monitoring, including bearing and motor winding temperatures, is an absolute must for high energy or high speed turbomachinery trains. It was felt that, had the installation of the vibration monitoring system been completed and armed for shutdown, equipment damage would have been greatly reduced. This incident initiated an investigation into the need to retrofit continuous monitoring systems on old turbomachinery trains. Steps taken for machinery protection of the 8000 hp motor have been applied to other turbomachinery trains in our plant. Details of these steps are covered later.

INSTALLATION/MODIFICATIONS OF NEW MOTOR

In early January 1982, the new prototype 8000 hp motor was installed on the existing base plates. During the January 19 start-up, the motor experienced high vibrations (7.0 mils peak-to-peak). A team was recording all vital signs and diagnosed the sub-synchronous vibration as bearing oil whirl. Figure 10 is the vibration plot of the motor outboard (opposite coupling end) bearing. Notice that the amplitude of the half-speed vibration in the vertical mode is over twice the running speed amplitude. Figure 11 illustrates a half-speed vibration level above synchronous speed vibration in the vertical mode of the inboard (coupling end) bearing.

As a point of interest, no sub-synchronous vibrations were observed when the motor was shop tested or solo run on the compressor deck. It was not until the motor ran coupled to the

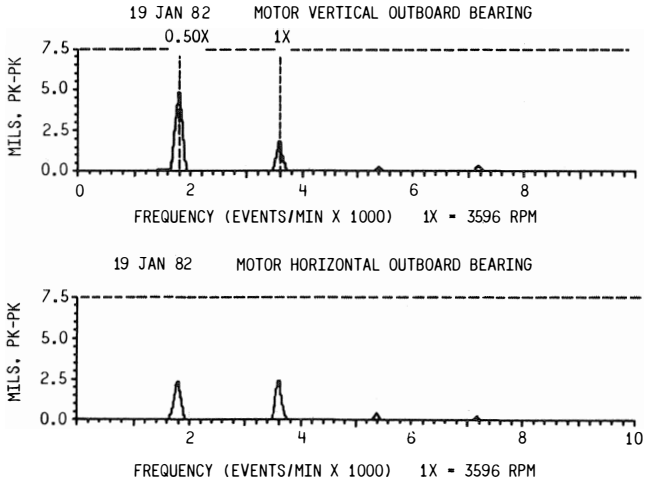

Figure 10. Start-up Vibration Data of 8000 hp Motor Outboard Bearing with 180° Design. Notice the Half Running Speed Vibration Level.

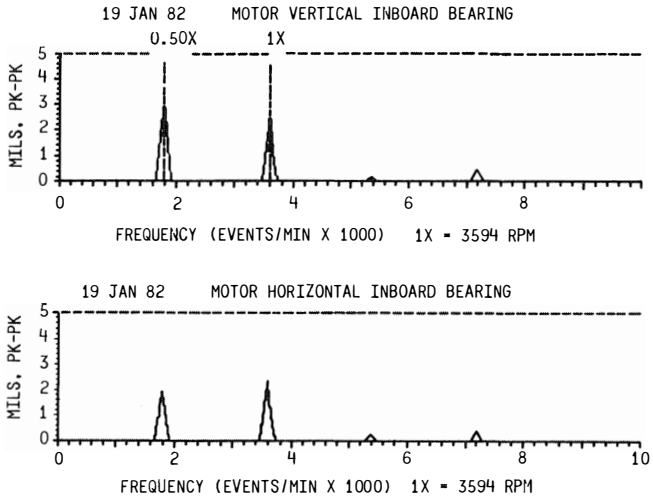

Figure 11. Start-up Vibration Data of 8000 hp Motor Inboard Bearing with 180° Design. Notice the Half Speed Vibration Level.

compressor via a 416 lb gear coupling that the sub-synchronous phenomena occurred.

The original motor bearings were of a ring lubricated 180° cylindrical design, with .014 in. design diametrical clearance. The existing bearings were modified to a full 360° cylindrical design by puddling babbitt into the bearing housings and machining the bores to .007 in. diametrical clearance. With the 360° plain journal bearings installed, the compressor was started up on January 23. Maximum motor vibrations of 1.2 mils were recorded on the coupling end in the horizontal direction. There was no evidence of sub-synchronous vibration at the time of start-up, as illustrated by Figure 12, so the unit was brought on-stream.

Because of the wreck and the start-up vibration problem with the new motor, the following actions were taken. The vibration monitoring system was made operational but not armed for shutdown. Vibration signals were transmitted to the control center computer to be stored for immediate retrieval with six-minute, hourly, and daily averages. Bearing temperatures (from embedded thermocouples), motor winding temperatures, motor amps, and oil pressure and temperature were also stored and trended by the process computer. Alert and danger vibration and temperature levels were established and programmed into the computer display. All vital equipment health information was available to the control board operator via video display.

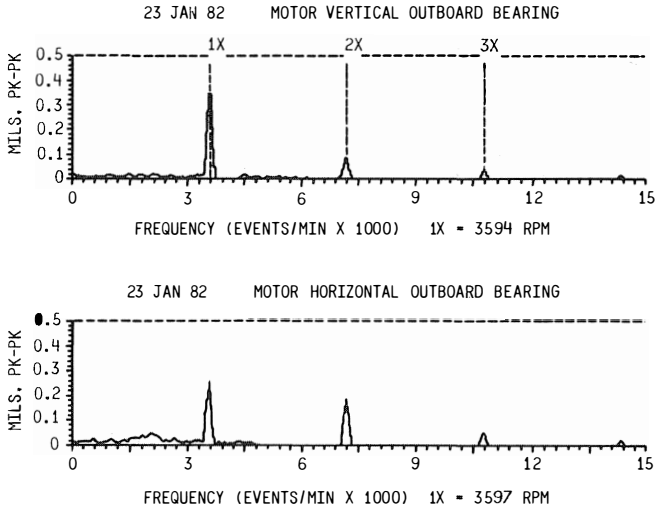

Figure 12. Start-up Vibration Data of 8000 hp Motor Outboard Bearing with 360° Design.

CYLINDRICAL BEARING OIL WHIRL

Close surveillance was maintained on the compressor train, even though all vital signs were normal. Plotting of vibration amplitudes, as illustrated in Figure 13, indicated a rising trend, which reached 2.0 mils in March. This increase occurred on the inboard end motor bearing in the horizontal direction. After reaching a peak of 2.0 mils, the vibration dropped to 1.6 mils and remained below 2.0 mils until mid-April. Orbital vibration displays would increase and decrease in diameter in a cyclic manner as if "winking at you" (see Figure 14). Continuing surveillance indicated a gradual increase in vibration levels, over a three month period, to a level of 2.6 mils (inboard bearing horizontal direction).

On June 19, during a routine check, the first correlation between increased vibration and operating parameters was detected. It was observed that a 3 psig fluctuation in the compressor deck oil supply header had caused an increase in the vibration level, which also contained a small sub-synchronous (half speed) component. This phenomenon occurred on the motor inboard bearing in the vertical direction. Further observations indicated the motor's sensitivity to ambient temperatures, which caused an increase in vibration levels in the morning and a decrease in the afternoon. This led to the false belief that the sun's heat was causing coupling misalignment. A cover was constructed to shade the motor, but this did not reduce the vibration.

The vibration alert limit of 3.0 mils was reached on July 25, with a maximum vibration of 3.6 mils at the inboard motor bearing. Both the vertical and horizontal readings were at 3.6 mils, with a large 1800 cpm sub-synchronous component. Prior vibration excursions had lasted only a short time, but this one continued for 5½ hours. At the time of the excursion, there was a change in both the oil supply temperature and the motor amps. Data indicated that a change in one or two of the operating parameters would not cause the apparent bearing oil whirl. The major "trigger factor" appeared to be "coupling lock-up," combined with variations in the operating parameters. Coupling lock-up was impossible to prove while the

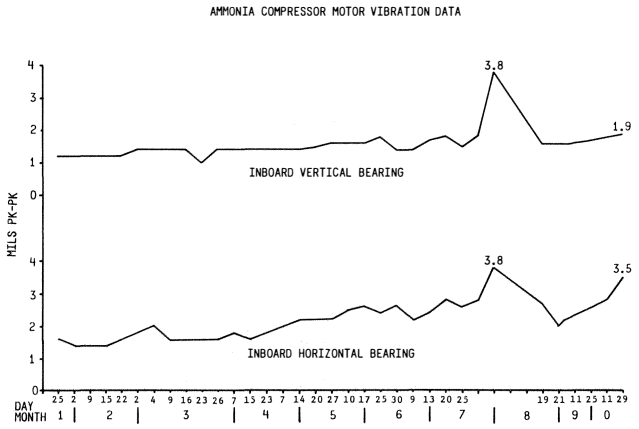

Figure 13. Ammonia Compressor Motor Vibration for 1982.

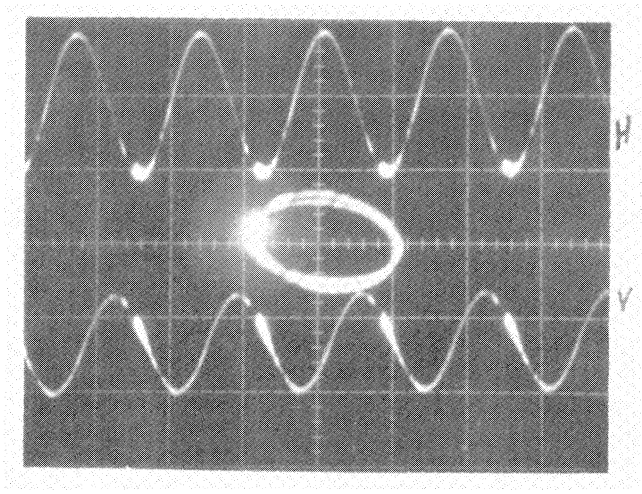

Figure 14. Orbital Display of Inboard Bearing Vibration. Notice the Orbit Fluctuation.

compressor train was running, but a history of short coupling life made it the number one suspect.

Final correlation was made on September 25, when a process problem caused a reduction in load on the ammonia compressor. A 49 amp change in motor load apparently caused the coupling to lock up and increased the inboard motor horizontal vibration to 2.6 mils (see Figure 15). When the vibration went to this level, the half-speed sub-synchronous component appeared. Figure 16 illustrates 1800 cpm vibration levels (in the inboard motor bearing, vertical direction), larger than synchronous speed vibration amplitudes. Figure 17 is a display of the inboard motor bearing vibration in the horizontal direction. Figure 18 is a computer print-out correlating inboard motor bearing vibrations, motor amps, and lube oil supply temperature. Computer stored vital signs data are a powerful diagnostic tool when trying to solve turbomachinery problems.

The September 25 excursion lasted only twelve minutes: normal vibration levels were regained when the motor amps were increased and the oil temperature lowered. At this point, the vibration monitor was armed for shutdown at 6.0 mils. The monitor was hard-wired for a two event shutdown. This would require the alert limit in the vertical and the danger limit in the horizontal direction, or vice versa, to be activated prior to a shutdown.

It was decided to make a computer model of the existing motor bearing and rotor system to simulate the oil whirl

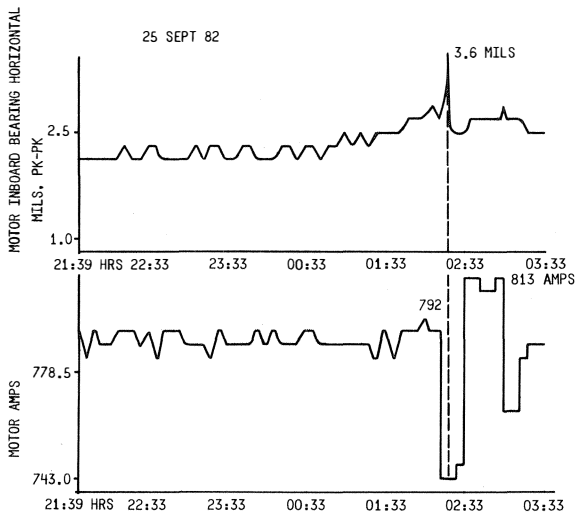

Figure 15. Historical Trend of Inboard Motor Bearing Vibration and Motor Load.

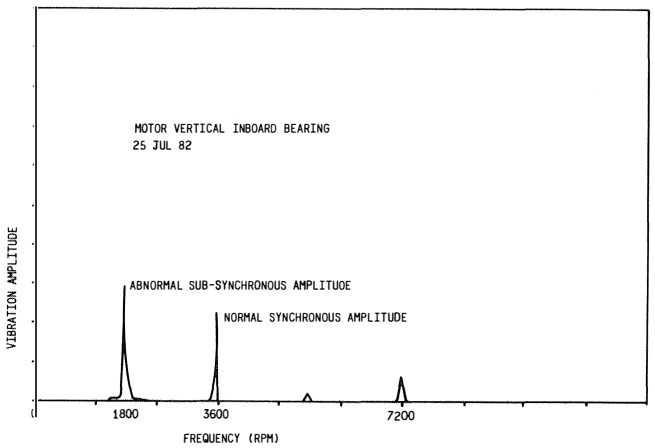

Figure 16. Inboard Motor Bearing Vibration Data in Vertical Direction. Notice High Sub-Synchronous Vibration.

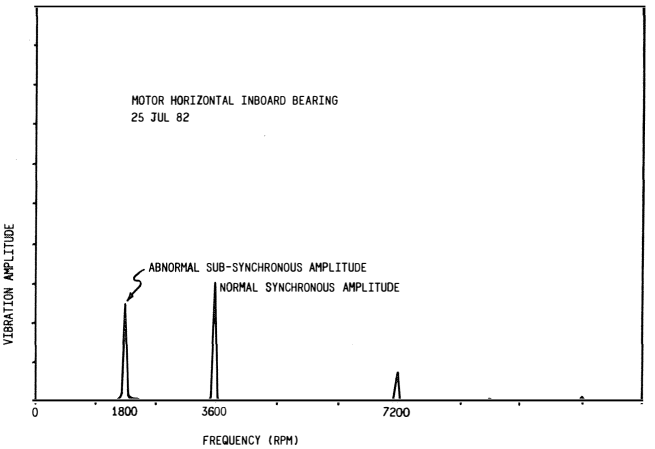

Figure 17. Inboard Motor Bearing Vibration Data in Horizontal Direction. Notice High Sub-Synchronous Vibration.

phenomenon. If the computer model did predict an oil whirl problem, the computer would be used to design and optimize a replacement bearing. Centritech Corporation was contracted to do the computer analysis and optimized bearing fabrication.

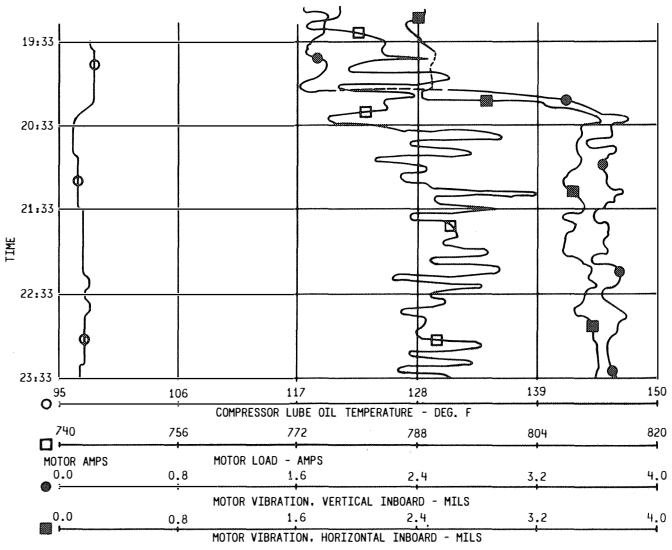

Figure 18. Historical Trend of Inboard Motor Bearing Vibration, Motor Amps, and Lube Oil Temperature. Rev. "A."

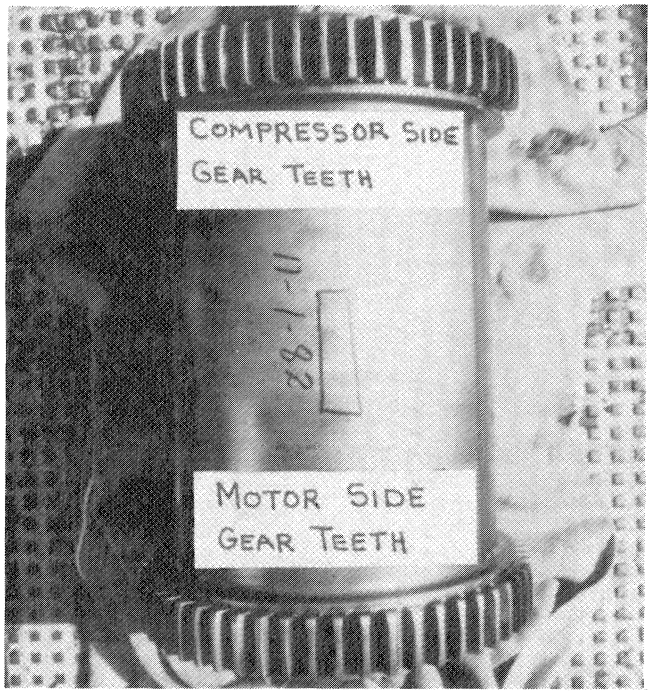

Figure 19. Teeth on the Coupling Spool Piece Showed Excessive Wear for a Nine Month Run.

Field data and suspicions, as well as the time frame for computer modeling and bearing fabrication, were passed on to Centritech's rotor dynamist. Computer modeling was to be completed within four weeks, and the bearings to be ready for installation by December 1.

Contact was made with the motor manufacturer during the early stage of the vibration problem. Information exchange occurred during the entire duration of the problem, so when dimensional data for the rotor and bearings were needed, there was full cooperation. A speedy solution to a serious problem was obtained because the familiar phrase "proprietary information" was not used. Detailed drawings of the rotor and bearings were furnished to Centritech to aid in developing the computer model. This was a big help in completing the computer analysis in time for the bearings to be manufactured and installed during a unit outage.

The only bearing design restraint was that of fitting the existing bearing support housing. Both bearings were to be insulated and to provide clearance for non-contact vibration probes. A 20 psig oil supply would be provided for top entry at each bearing if required. Bearing clearances were to be set and checked by the vendor, with the bearing to be installed by the customer.

COUPLING DAMAGE

On October 29, 1982, the ammonia compressor train was shut down because of high product inventory. While the computer analysis was being performed, a unit turnaround began. Examination of the gear coupling after a nine-month run indicated heavy tooth wear and one broken tooth on the compressor side. Figure 19 shows the coupling spool piece. Tooth wear on both the spool piece and shrouds was considered excessive for a nine-month run and probably was caused by poor lubrication. A metal chip was found lodged in the compressor side oil supply tube to the coupling (see Figure 20). The compressor side coupling teeth showed signs of pitting due to heavy loading and lack of lubrication. Figure 21 shows the broken tooth and pitting on the compressor side. Dark areas at the teeth wear lines of the compressor end shroud (Figure 22) indicated poor lubrication. Coupling wear on the motor side of the spool piece and shroud was excessive for a nine-month run, as illustrated by Figures 23 and 24. The motor shroud teeth indicated that some of the teeth were taking little or no load. Non-uniform loading of the teeth could have caused excessive wear and pitting. All coupling damage information was relayed to Centritech for correlation with the computer analysis.

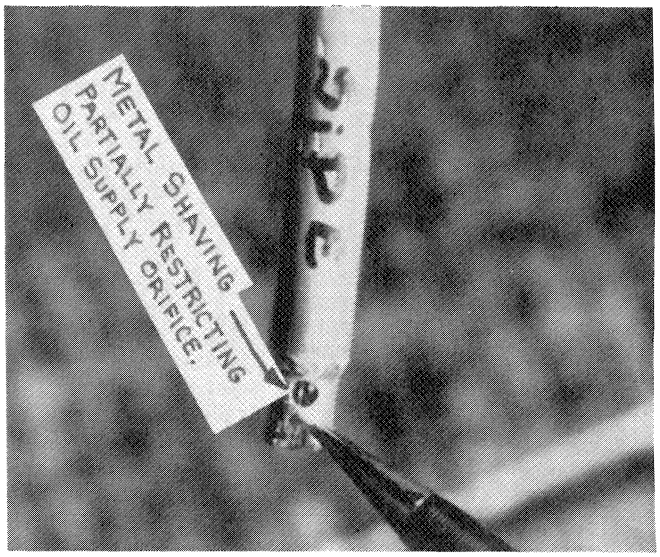

Figure 20. A Metal Shaving Was Found Lodged in the Compressor Side Coupling Oil Supply Nozzle.

ROTOR DYNAMICS ANALYSIS

The original motor rotor, shown in Figure 25, has a 4,661-lb rotating element. The rotor is supported in two plain cylindrical journal bearings, with a span of 91.65 in. Both journal diameters are 3.994 in.

The motor shaft is constructed by mounting a laminated core on a 10.0-in. diameter shaft section. The core is 39.0 in. long and 22.12 in. in diameter. Because the effective stiffening

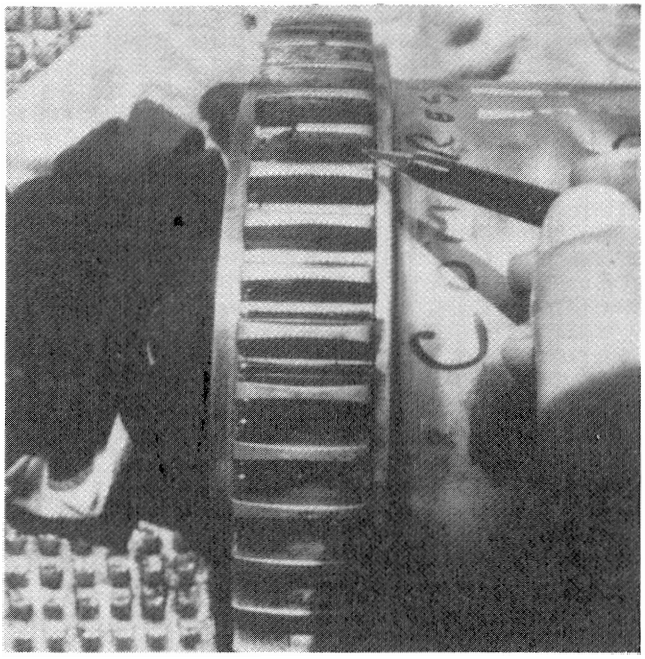

Figure 21. A Broken Tooth and Heavy Tooth Pitting Were Found on the Compressor Side of the Spool Piece.

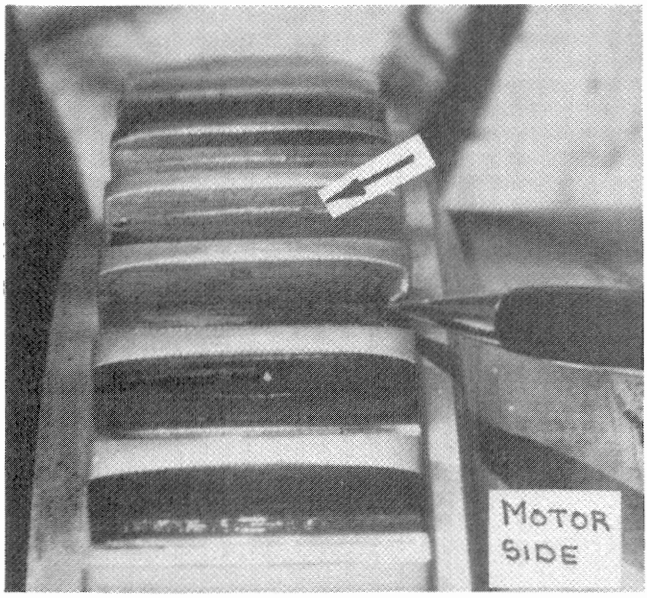

Figure 23. Motor Side Coupling Spool Piece Gear Teeth Showed Excessive Wear for Only Nine Months of Service.

Figure 22. Compressor Side Coupling Shroud Gear Teeth Showed Excessive Wear for Only Nine Months of Service.

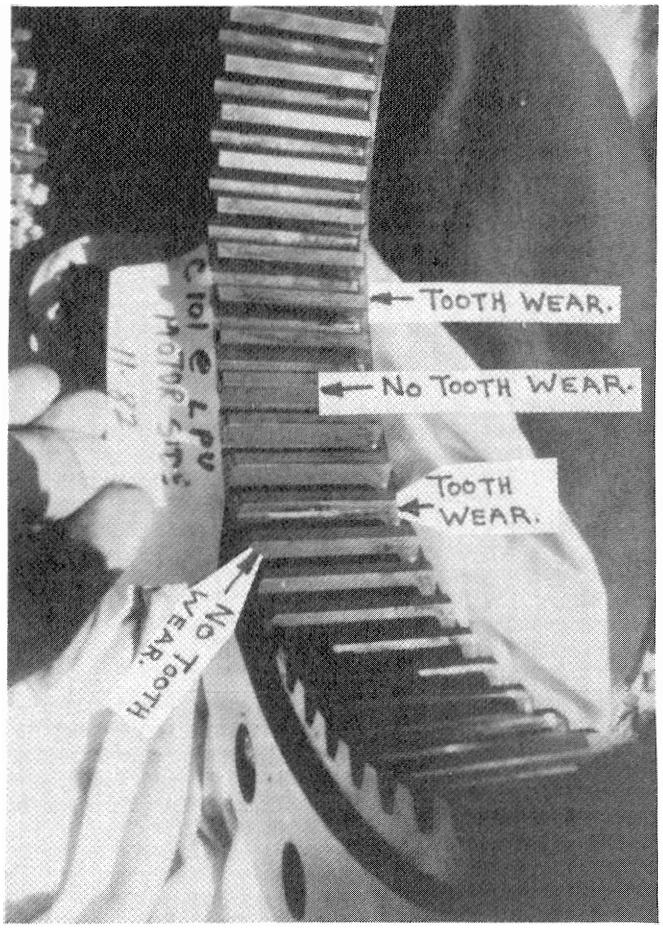

Figure 24. Motor Side Coupling Shroud Gear Teeth Indicated Some Teeth Were Taking Little or No Load.

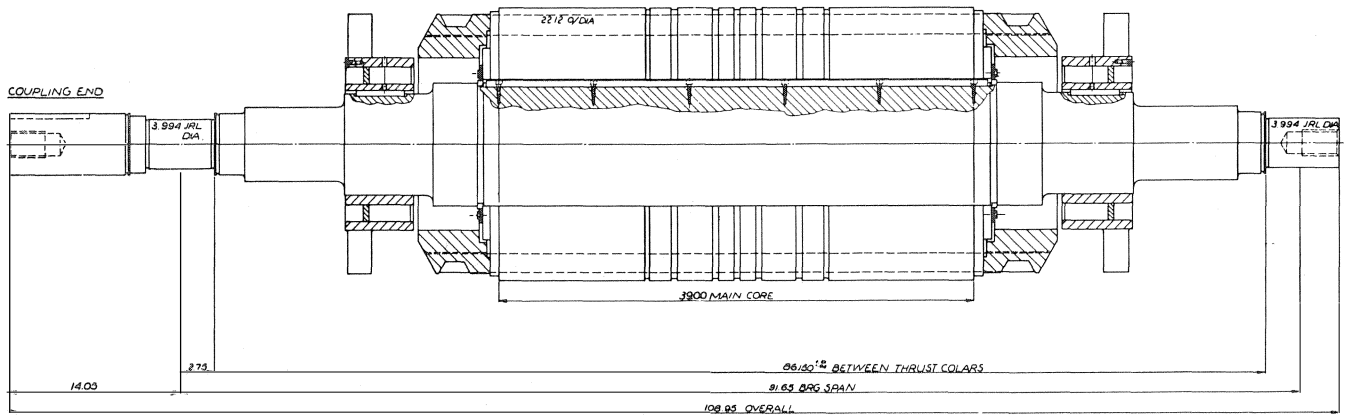

Figure 25. Induction Motor Rotor.

contribution of the core was not known, the model was evaluated using two extreme conditions for the main core section stiffness. The philosophy behind this approach is that these two extremes would bracket the actual rotor dynamic characteristics. The first extreme is referred to as the "unstiffened" condition. This includes the weight, but not the stiffening contribution of the core. Therefore, the shaft stiffness in the core section considers only the 10.0-in. diameter shaft. The second extreme is referred to as the "stiffened" condition. This includes the weight and the bending moment of inertia of the 22.12 in. diameter core section. Therefore, the area moment of inertia of the stiffened section is 11,752 in^4.

Note that consideration was given to back-calculating for effective shaft diameter from measured frequencies. However, this technique can be misleading if a measured frequency on rigid supports is not available.

The rotor assembly is modeled as a series of lumped mass stations containing the weight and inertia properties of the motor core, coupling, etc. These mass stations are mathematically interconnected by elastic shaft elements. The rotor model also contains the bearing support locations, with speed-dependent stiffness and damping properties of the oil film.

Figure 26 is the computer-generated shaft cross section plot, indicating the division of the rotor shaft into discrete sections. Each section line indicates a mass station.

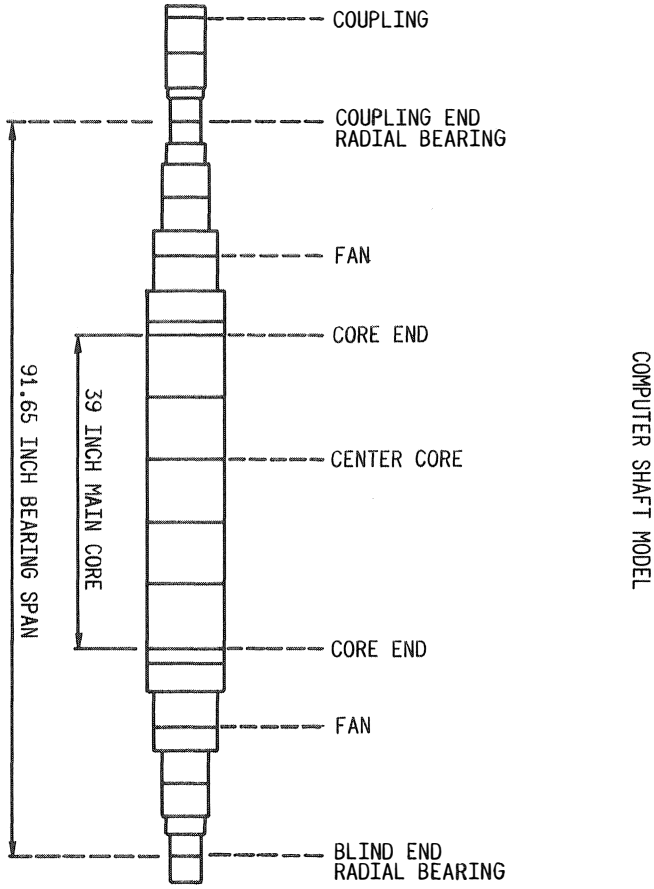

Figure 26. Computer Shaft Model.

ANALYTICAL PREDICTION OF EXISTING SYSTEM CHARACTERISTICS

Undamped Critical Speeds

Figure 27 is the critical speed map for the original rotor, with the existing coupling. The solid lines show the criticals with an unstiffened core section.

Figures 28 and 29 are first undamped critical speed mode shapes for the unstiffened rotor, considering arbitrary bearing stiffnesses of 1×10^6 and 1×10^8 lb/in. The two bearings are assigned the same stiffness values, as indicated in the figure title. Note that Figure 28 shows a large percentage of bearing motion, because a bearing stiffness of 1×10^6 lb/in is quite flexible, compared to the rotor shaft stiffness. If the bearing stiffnesses are increased to 1×10^8 lb/in, Figure 29 shows no bearing motion. This represents the rigid bearing case, in which the bearings have become far too stiff for the rotor. In this condition, the rotor has no effective bearing damping, because there is no bearing motion. Referring to the critical speed map, one can see that this condition would occur at bearing stiffnesses above 6×10^6 lb/in. Therefore, an alternate bearing design must not exceed this bearing stiffness value at the first critical speed, in order to allow safe operation through this mode.

Figures 30 and 31 illustrate these mode shapes when the rotor core stiffening effect is included. Note the resistance to bending in the stiffened core section. This stiffening increases the critical speeds, as indicated on the map.

Existing Plain Journal Bearings

The existing bearings, shown schematically in Figure 32, are plain cylindrical journal bearings consisting of two lands, separated by a circumferential groove. These bearings were designed for oil ring lubrication, as shown in Figure 33.

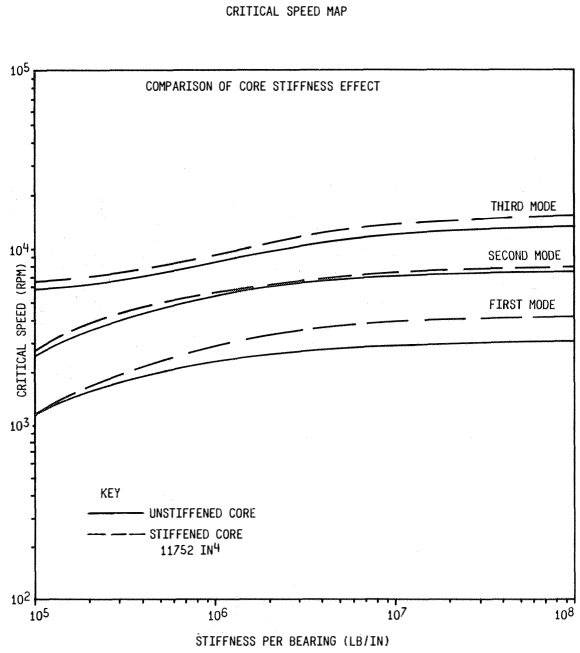

Figure 27. Critical Speed Map.

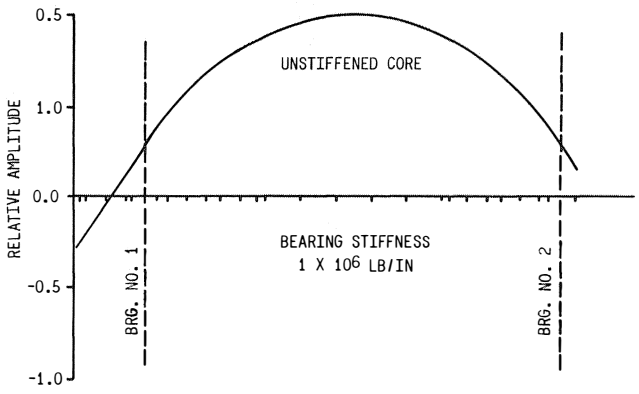

Figure 28. First Mode Shape with Unstiffened Core and Flexible Bearings.

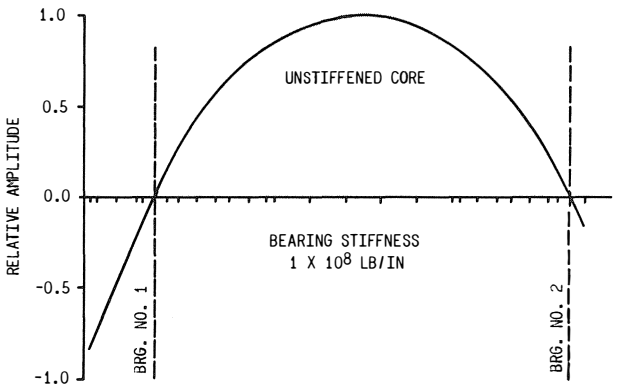

Figure 29. First Mode Shape with Unstiffened Core and Rigid Bearings.

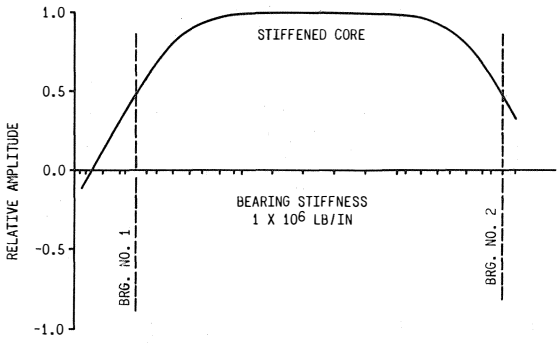

Figure 30. First Mode Shape with Stiffened Core and Flexible Bearings.

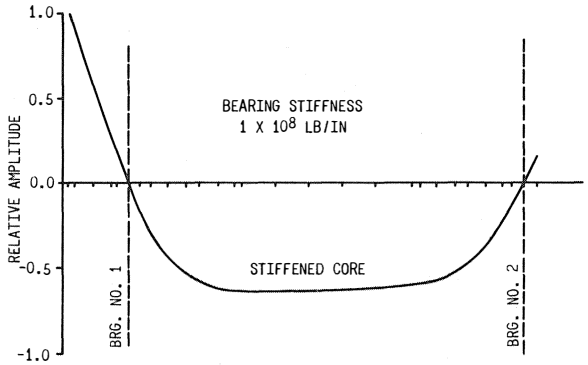

Figure 31. First Mode Shape with Stiffened Core and Rigid Bearings.

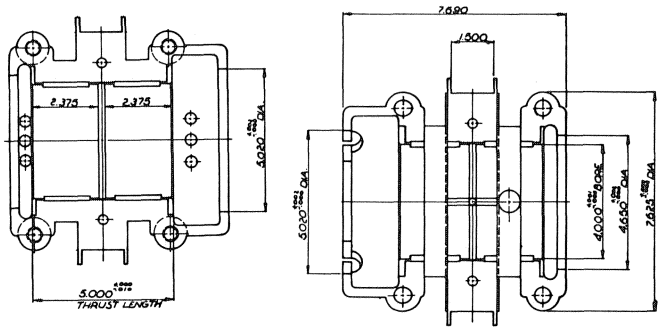

Figure 32. Original Plain Bearing Design.

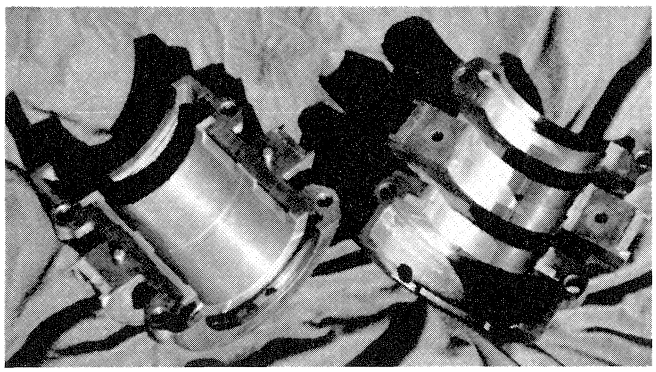

Figure 33. Original Oil Ring Lubricated Plain Journal Bearings.

Therefore, a portion of the top half is removed for the oil rings. However, the analysis assumes a 360° plain cylindrical journal bearing with oil distribution grooves at the split line. The double land is included by considering one half of the bearing load on one land. Then, each bearing consists of two "land" bearings in parallel.

The existing oil is rated at 154.5 SSU @ 100°F and 44.3 SSU @ 210°F. Oil inlet temperature is 97-100°F. Therefore, the outlet temperature for a 30°F rise is 130°F.

Figure 34 contains a cross-plot of the original bearings on the critical speed map for a bearing clearance of 0.007 in. Table 1 lists these intersections, which are the undamped critical speeds.

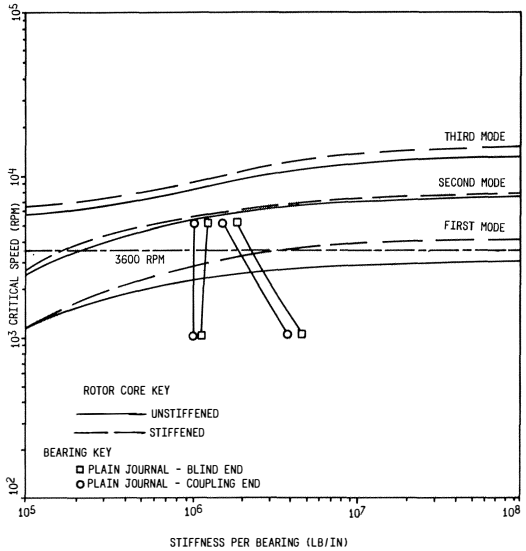

Figure 34. Critical Speed Map with Original Bearings.

Table 1. Undamped Critical Speeds with Original Bearings.

	Unstiffened Core	Stiffened Core
Horizontal (X)	2,200 - 2,250 rpm	2,750 - 2,850 rpm
Vertical (Y)	2,450 - 2,500 rpm	3,150 - 3,200 rpm

Synchronous Unbalance Response

A synchronous unbalance response analysis was performed to determine the peak response speeds and amplitudes for the stiffened and unstiffened models. The analysis indicated that the core stiffening does have a significant effect on bending in the core section. This is shown in Figure 35.

Bearing Stability

This is an initial assessment to evaluate the ability of the existing bearings to provide stable rotor support, without considering flexible rotor effects. It is a parametric analysis to search for potential stability problems. Therefore, an approximate bearing load of one half the rotor weight was assumed. The actual bearing loads are considered later in the analysis. Three effects were considered: oil temperature, bearing clearance, and bearing unloading.

Table 2 lists bearing stability as a function of oil temperature. The assumed temperatures are 110, 130 and 170°F. Note that oil temperature has a significant effect on viscosity. For this oil, an increase of 60°F reduces the viscosity by a factor of 3. The table shows that the bearing stability remains relatively

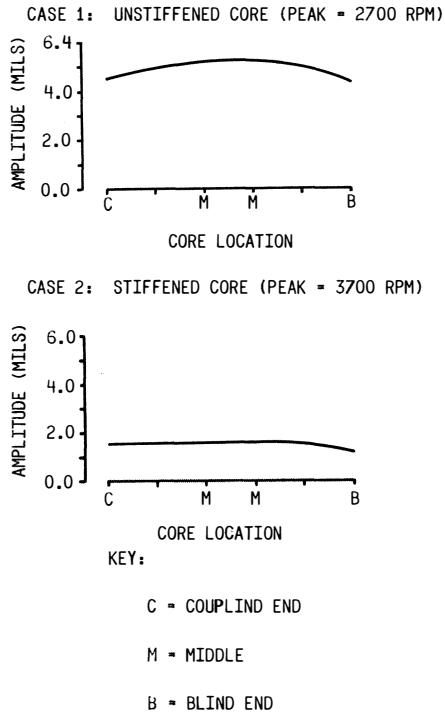

Figure 35. Peak Response Amplitudes in Motor Core.

Table 2. Effect of Oil Temperature on Original Bearing Stability.

Oil Temperature (°F)	Oil Viscosity (reyns)	% Margin from Threshold	Stability
110	3.174×10^{-6}	48% Below	Stable
130	2.03×10^{-6}	47% Below	Stable
170	1.08×10^{-6}	50% Below	Stable

constant over this temperature range.

Table 3 lists bearing stability versus a clearance range of 0.006 to 0.014 in. The percent from threshold indicates some sensitivity to clearance, but these results are not too conclusive.

Table 4 lists bearing stability versus unloading force for a bearing clearance of 0.007 in. The table indicates a significant loss of stability at higher unloading conditions. Note in particular that Table 4 shows a marked loss of stability for an 800 lb unload force. When the unloading force reaches 1,600 lb (69% of gravitation load), the bearing is only marginally stable. Finally, a run was made considering the actual gravity bearing load and a 1,600 lb unload, with the result that the bearing was on the threshold of stability. Therefore, the bearing stability is indeed sensitive to unloading.

The bearing stability sensitivity to unloading is a cause for concern, because external unloading is highly possible. There are two primary sources of unloading force: misalignment between the motor and the compressor, and electromagnetic forces between the rotor and stator.

The next step is to examine stability of the flexible rotor supported in these bearings. Emphasis will be on the effects of unloading on rotor system stability.

Table 3. Effect of Clearance on Original Bearing Stability.

Diametral Clearance (in.)	% From Threshold	Stability
0.006	51% Below	Stable
0.007	47% Below	Stable
0.008	44% Below	Stable
0.010	49% Below	Stable
0.014	45% Below	Stable

Table 4. Effect of Unloading on Original Bearing Stability.

Unload per Bearing	% from Threshold	Stability
0	47% Below	Stable
400	42% Below	Stable
800	35% Below	Less Stable
1600	8% Below	Marginally Stable
1600*	0%	Threshold

*The 1600 lb unload case is even more dramatic with final design load. The final design load at coupling end bearing was 2,168.4 lb.

Flexible Rotor Stability

Flexible rotor stability is assessed by calculating the system damped eigenvalues. The damped eigenvalue ($s = \lambda + i\omega_1$) is a complex number composed of a real part (λ), which is the growth factor, and an imaginary part (ω_1), which is the damped frequency. The growth factor is the rate of exponential decay (or growth) of the vibration amplitudes. If λ is positive, the vibration grows with time, and the system is unstable. If λ is negative, the vibration decays with time, and the system is stable.

The log decrement (δ) is a standard non-dimensional indicator of stability of a system. It represents the natural log of the ratio of two successive amplitudes of system vibration and is computed from the complex eigenvalues as $\delta = -2\pi\lambda/\omega_1$. If δ is positive, the system is stable. If δ is negative, the system is unstable.

Tables 5 through 7 are flexible rotor stability tabulations. Bearing gravity loads are approximated at 50% of the rotor weight. Rotor core stiffening is not included.

Table 5 lists rotor stability versus oil temperature for a clearance of 0.007 in. These results indicate the same insensitivity that was found for the bearing stability assessment. It should be noted that the log decrements of 0.16 and 0.12 are all low. Therefore, this is not a highly stable system to begin with.

Table 6 shows a very definitive down-grade in stability at larger bearing clearances. At a clearance of 0.014 in., the log decrement of 0.04 indicates that the rotor is near the threshold.

Table 5. Effect of Oil Temperature on Rotor Stability with Original Bearings and Unstiffened Core (Approximate Gravity Loads).

	Oil Temperature (°F)		
	110	130	170
Oil Viscosity (micro reyns)	3.17	2.03	1.08
Frequency (rpm)	2150	2160	2120
Log decrement	+0.16	+0.12	+0.12
Stability	Stable	Stable	Stable

Table 6. Effect of Bearing Clearance on Rotor Stability with Original Bearings and Unstiffened Core (Approximate Gravity Loads).

	Bearing Clearance (In.)			
	0.006	0.007	0.010	0.014
Frequency (rpm)	2,220	2,160	1,970	1,840
Log decrement	+0.16	+0.12	+0.14	+0.04
Stability	Stable	Stable	Stable	Marginal

Table 7. Effect of Bearing Unloading (Both Ends) on Rotor Stability with Original Bearings and Unstiffened Core (Approximate Gravity Loads).

	Unloading Force per Bearing (lb)			
	0	400	800	1600
Frequency (rpm)	2,160	2,070	1,980	2,480
Log decrement	+0.12	+0.11	+0.07	+0.03
Stability	Stable	Stable	Marginal	Marginal

Table 7 solidifies the initial concern about unload sensitivity. It was assumed that the bearing clearance was 0.007 in. and the oil temperature was 130°F. There are two important observations. First, the rotor stability is almost at the threshold for an unloading force above 800 lb per bearing. Second, the whirl frequency drops to 1,980 rpm for an 800 lb unload. This is very close to the observed whirl frequency, near 1,800 rpm, that was observed in field data. This coincidence justified refinement of the assumptions in order to further pursue this unloading phenomenon.

Table 8 is the final stability tabulation, assuming two different clearances for both rotor core models. These results were obtained using actual bearing gravity loads, instead of the approximate 50% assumption. Also, note that the unloading is only considered to act at the coupling bearing. The blind-end bearing is loaded by gravity in all cases. The unloading only at the coupling bearing is more closely representative of misalignment loads due to a locked coupling. Four observations are important: First, stability frequencies and log decrements are on the same order of magnitude for either clearance. However, stability at a clearance of 0.007 in. is slightly less than at 0.006 in. Second, stability is much higher, with no unloading, when core stiffening is included. Log decrements of +0.7 and +0.5 are very stable values. Third, core stiffening does not eliminate

rotor instability with bearing unloading. The unstiffened model is unstable (log decrement = −0.16) when the coupling bearing is unloaded by 1,600 lb. The stiffened model is marginally stable (log decrement = +0.07) for this assumed unloading condition. Fourth, both core stiffness assumptions yield unstable whirl frequencies near 1,800 rpm. Therefore, this unloading phenomenon is highly suspected.

BEARING OPTIMIZATION

Proposed New Design

Figure 36 shows the new proposed tilt pad bearings, and Figure 37 shows a comparison of the original and new bearings. The new bearings, shown again in Figure 38, are of a four shoe tilting pad design, with L/D of 1.0, preload of 0.33, and orientation load-between-pad. This design incorporates ball and socket pivots, which can be seen in Figure 39.

The stiffness coefficients for the new tilt pad bearings are shown on the critical speed map for the existing rotor in Figure 40.

Table 9 lists the intersections of the new bearing stiffnesses and the critical speed curves, which represent the undamped critical speeds with the new tilt pad bearings.

Comparison of Original and Conversion Bearings

A straddle mount rotor with a relatively symmetric weight distribution can be approximated as a single mass rotor in order to assess the effect of different bearings on the rotor dynamics near the first critical speed. These quantities are only approximations, based on the first mode of the rotor [1].

With the rigid bearing critical speed (ω_{cr}) and modal weight (M_m), the effective shaft stiffness is expressed as

$$K_s = \omega_{cr}^2 M_m$$

The total critical bearing damping can also be calculated as

$$C_{cr} = 2 M_m \omega_{cr}$$

Table 8. Flexible Rotor Stability Original Plain Journal Bearings (Final Gravity Loads).

Bearing Clearance (in.)	*Bearing Load*	*Frequency (rpm)*	*Log Decrement*	*Stability*
CASE A: UNSTIFFENED CORE:				
0.006	Gravity	2,193	+0.16	Stable
0.007	Gravity	2,134	+0.13	Stable
0.007	1,600 lbs (unload at coupling end only)*	1,739	−0.16	Unstable
CASE B: STIFFENED CORE:				
0.006	Gravity	2,658	+0.74	Very Stable
0.007	Gravity	2,542	+0.54	Very Stable
0.007	1,600 lbs (unload at coupling end only)*	1,864	+0.07	Marginal

*Gravity load at blind end

Table 9. First Undamped Critical Speed (rpm) with New Tilt Pad Bearings.

Oil Type	Unstiffened Core	Stiffened Core
Light, ISO 32	2,400	3,100
Heavy, ISO 68	2,300	2,950

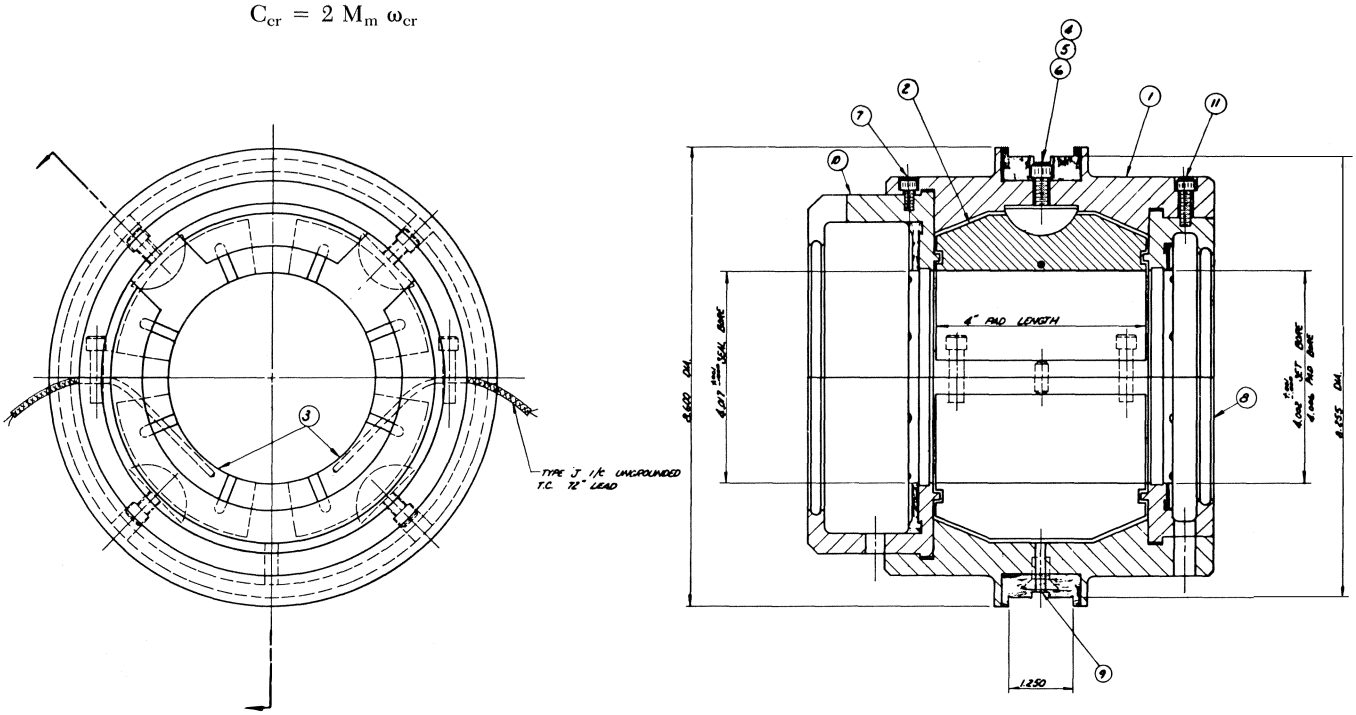

Figure 36. New Tilt Pad Bearing Design.

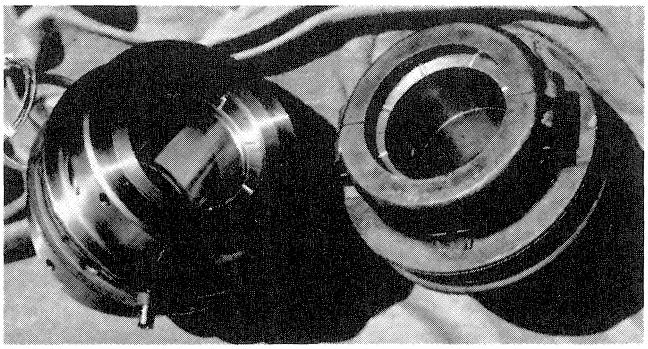

Figure 37. Original Bearing (left) and New Bearing.

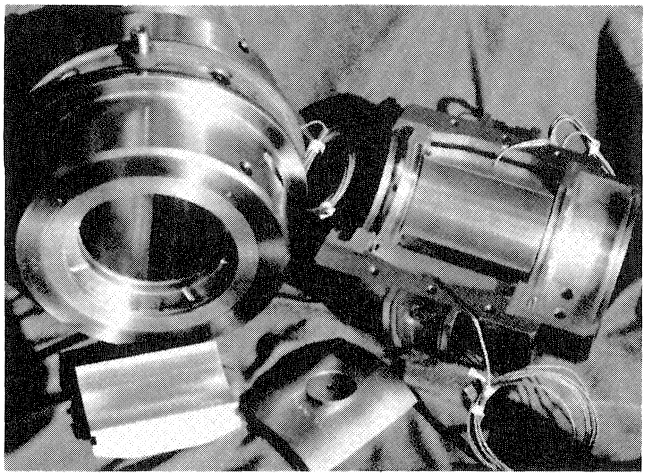

Figure 38. New Tilt Pad Journal Bearing—Four Pad Design.

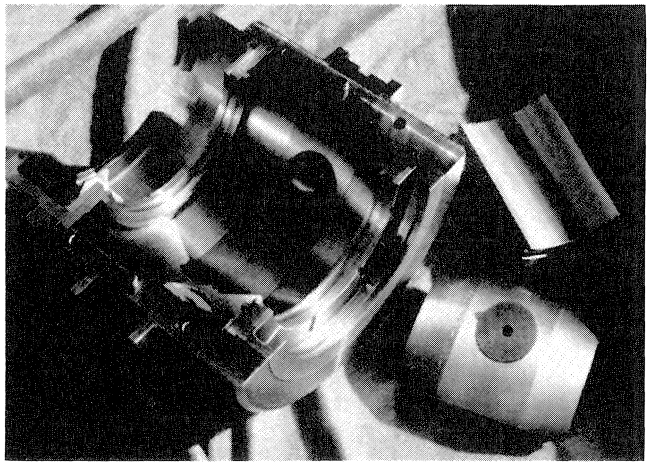

Figure 39. New Bearing Showing Ball and Socket Pivots Behind Pads.

These quantities are used in the calculation of two important non-dimensional rotor/bearing design parameters, called stiffness and damping ratio.

The stiffness ratio is the total bearing stiffness divided by the rotor stiffness, or

$$\bar{K} = (K_{b1} + K_{b2}) / K_s$$

where

K_{b1} and K_{b2} = stiffness values for each of the bearings

The optimum value for this ratio is 6 or less.

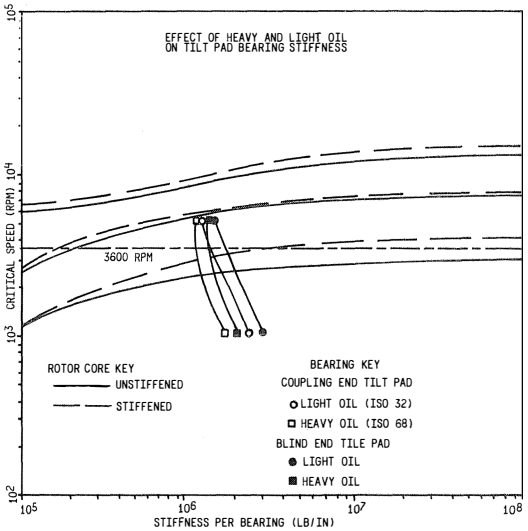

Figure 40. Critical Speed Map with New Bearings.

The damping ratio is the total actual bearing damping divided by the total critical damping [1], or

$$\xi_{act} = (C_{b1} + C_{b2}) / C_{cr}$$

where

C_{b1} and C_{b2} = damping values for each of the bearings

This ratio is compared to the optimum damping ratio, which is approximated from the stiffness ratio as

$$\xi_{opt} = (1 + \bar{K}) / 2$$

It should be noted that these ratios can be calculated for both the horizontal and vertical directions. However, only the vertical (γ) direction is presented here, for illustration purposes, because the gravitational rotor load causes the vertical stiffness to be higher than the horizontal stiffness. Therefore, the vertical stiffness must be carefully monitored in assessing different bearing selections.

The rigid bearing critical speed is 2,630 rpm without core stiffening and 3,720 rpm with core stiffening. Therefore, the rotor shaft stiffness is 4.6×10^5 lb/in without core stiffening and 9.2×10^5 lb/in with core stiffening. The critical damping values without and with stiffening are 3,318 and 4,708 lb/sec/in. These quantities were used to compute the stiffness and damping parameters presented in Table 10. Note that the original stiffness ratios were 10.7 and 5.3 for the unstiffened and stiffened conditions, respectively. With the new bearings, these values are reduced by 46%, and both are below the recommended value of 6.0. The new bearing stiffness curves cross the first mode curve below the rigid bearing limit. Figure 40 shows that the new bearing stiffnesses cross the critical speed curve between 1×10^6 and 2×10^6 lb/in.

Table 10 also presents a comparison of actual and optimum damping ratios for the existing plain journal bearings and the new tilt pad bearings. Note that the original bearings were overdamped. The actual damping ratio is 200-271% of the optimum. The new tilt pad bearings are significantly better, providing 96-119% of optimum damping.

Table 10. Bearing Comparison.

	Core Stiffness Assumptions (lb/in)	
	Unstiffened 4.56×10^5	Stiffened 9.18×10^5
Case A: Original Bearings*		
Stiffness Ratio:		
K (DIM)	10.7	5.3
Actual Damping Ratio:		
ξ_{ACT} (DIM)	12.2	8.6
% ξ_{OPT}	209	271
Optimum Damping Ratio:		
ξ_{OPT} (DIM)	5.85	3.2
Case B: New 4 pad TPJ**		
Stiffness Ratio:		
K (DIM)	5.8	2.9
Actual Damping Ratio:		
ξ_{ACT} (DIM)	3.3	2.3
% ξ_{OPT}	96	119
Optimum Damping Ratio:		
ξ_{OPT} (DIM)	3.4	1.9

*Clearance = 0.007, ISO 32 Oil

**L/D = 1.0, Preload = 0.33, ISO 68 Oil

ANALYTICAL PREDICTION OF MODIFIED SYSTEM CHARACTERISTICS

Synchronous Unbalance Response

The unbalance response analysis [2, 3] indicated satisfactory operating characteristics with the new tilt pad journal bearings.

Flexible Rotor Stability

Table 11 indicates the flexible rotor stability [4, 5] with the new tilt bearings. The system is very stable with ISO 32 oil: the log decrements are +0.31 and +0.67 for the stiffened and unstiffened core assumptions, respectively. With ISO 68 oil, these log decrements increase to +0.45 and +0.89. Therefore, the heavier oil provides even greater stability.

Table 11. Flexible Rotor Stability with New Tilt Pad Bearings (3600 rpm).

Oil Type	Core	Frequency (RPM)	Log Decrement	Stability
ISO 32	Unstiffened	2,400	+0.31	Stable
	Stiffened	3,220	+0.67	Very Stable
ISO 68	Unstiffened	2,408	+0.45	Very Stable
	Stiffened	3,290	+0.89	Very Stable

System Stability

This analysis has shown that the existing rotor-bearing system in plain journal bearings is marginally stable with no core stiffening. The log decrement is only +0.13 for a bearing clearance of 0.007 in. However, with the stiffened core assumption, the original system is very stable. The log decrement increased to +0.5 for a bearing clearance of 0.007 in.

The key to understanding this system is that it has an inherent weakness to become unstable due to the following influences:

1. Bearing clearance—The rotor system is marginally stable for bearing clearances on the order of 0.014 in.
2. External bearing unloading—There are external forces that oppose gravity loading, with two primary examples:
   a. electromagnetic forces between the rotor and stator
   b. misalignment loads transmitted through the coupling

In fact, the system stability is sensitive, regardless of whether or not the core stiffening is included. If a 1,600 lb upload is exerted at the coupling end bearing, the log decrements are −0.16 with the unstiffened core and +0.07 with the stiffened core.

Therefore, the core stiffening effect that made the dramatic difference without external unloading does not ensure stability under the influence of external forces. These analytical findings provide a logical explanation for the rotor instability problem measured in the field. The other important correlation is that the unloaded case yields whirl frequencies of 1,739 rpm and 1,864 rpm for the two core stiffness assumptions. The whirl instability measured in the field was 1,800 rpm. This rotor whirl problem is compounded by the fact that the whirl frequency is at half running speed. The analysis also showed that the coupling bearing is on the whirl threshold for a 1,600 lb upload. Therefore, half frequency whirl is likely under the circumstances.

The loss of stability due to external forces leaves this unit vulnerable to another destabilizing mechanism, called internal friction. Recall that the long rotor core section is a separate component that is mounted on the shaft with a light interference fit. When relative sliding occurs between the base shaft and core, internal friction is created. The impact of this behavior is that the sliding action is a deflection-dependent destabilizing mechanism that can cause hysteretic whirl. The deflection dependence could also help explain the self-perpetuating whirl amplitude excursions that occurred in the field.

A new set of journal bearings was designed to eliminate the instability problem and to minimize synchronous vibration. The optimum bearing is a four shoe tilting pad type. The bearings are identical on both ends of the machine. The geometry is L/D = 1.0, preload = 0.33, and set clearance = 0.008 in., and the orientation is load-between-pad. It is also recommended that the oil be changed to ISO 68.

Motor Inspection and Bearing Installation

On December 2, 1982, the top end bells of the motor were removed to install the new tilting pad bearings. This action revealed an oil soaked stator and rotor. A loose connection on the pressure balancing line from the motor fan shroud to the bearing labyrinth seal housing had allowed oil to be sucked into the eye of the fan. Once at the eye of the fan, the oil was circulated throughout the stator and over the rotor. Even though the loose connection was on the coupling end bearing, the outboard end of the motor was also oil soaked (see Figure 41).

Since the motor was still under warranty, the manufacturer's local representative was contacted. The motor was taken to their authorized repair center for inspection and cleaning. A detailed repair list was developed by our rotating equipment specialist and sent with the motor. Complete details of the inspection and repairs will not be covered in this paper. It should be mentioned that, during the inspection, the rotor was chucked in a lathe with one end on a steadyrest bearing for a mechanical runout check. The mechanical runout indicated a .004 in. bent shaft, starting at the rotor side of the coupling end

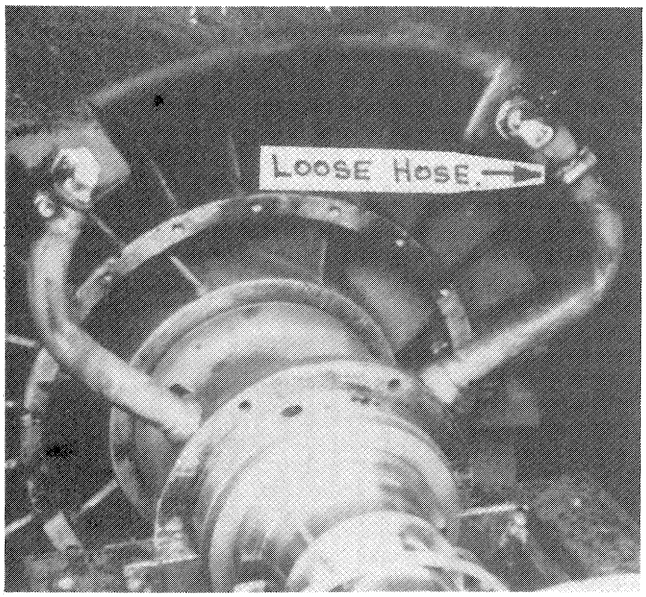

Figure 41. A Loose Pressure Balancing on the Coupling End of Motor Caused Bearing Oil to be Sucked into the Windings.

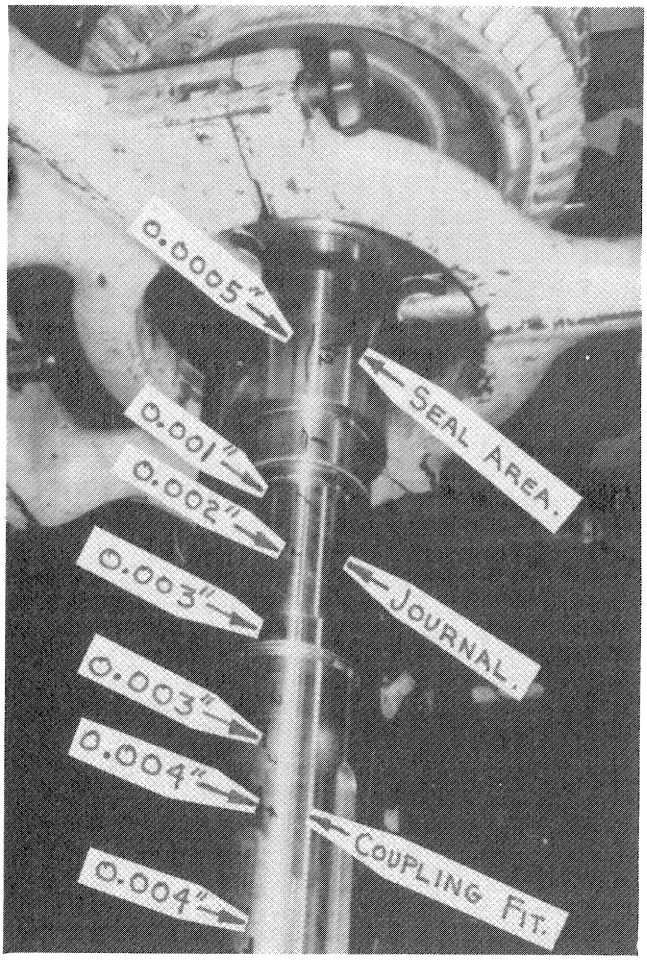

Figure 42. Runout Check of Motor Rotor Indicated a Bent Shaft Starting at the Bearing Journal.

bearing journal and running to the end of the shaft (see Figure 42). Since the shaft was made from heat treated 4140 steel and the bend was in the bearing journal, the decision was made to go with the .004 in. runout. If localized heat had been used to straighten the shaft, the heat treatment could have been affected, increasing the runout. Shaft straightening by peening would have damaged the bearing journal.

While at the shop, the new tilting pad bearings were installed and the rotor air gap checked. The air gap was the same for the tilting pad bearings as for the old cylindrical journal bearing.

Oil lines through the side of the motor were increased from ⅜ in. to ½ in. stainless steel pipe. A ⅝ in. polytetrafluorethylene (PTFE) lined, stainless steel braided, flexible hose connected each bearing to the oil supply through the side of the motor.

With the motor assembly completed, a reduced voltage (700 volts) full speed shop test was conducted on the old bearings. This was required because a pressurized oil supply was not available for the tilting pad bearings. Shaft vibrations were 1.4 mils peak-to-peak on the outboard bearing and 1.0 mil on the inboard. Electrical runout on both ends had been reduced to 0.5 mil by burnishing.

During the motor cleaning and bearing modification, a team of machinists drained and cleaned the 1500 gallon lube oil reservoir. Both oil filter housings were cleaned and filled with 25 micron filter elements. Centritech's recommendations for oil viscosity and temperature were followed. The lube oil reservoir was filled with an ISO 68 oil, and the oil temperature thermostat was changed from 120°F to 105°F. The entire lube oil system was checked and adjusted to maintain a 26 psig oil pressure.

Minor piping modifications were made to the motor and coupling oil supply and drain lines. Motor lube supply lines were increased from ⅜ in. to ¾ in. stainless steel pipes connected to the motor via PTFE-lined, stainless steel braided, flexible hoses (see Figure 43). It was necessary to increase the oil drain lines from ¾ in. to 1¼ in. to handle the increased bearing oil supply (see Figure 44). The oil supply line to the coupling was also increased in order to improve coupling lubrication. An inspection window was installed in the upper half of the coupling guard for visual check of oil flow (see Figure 45).

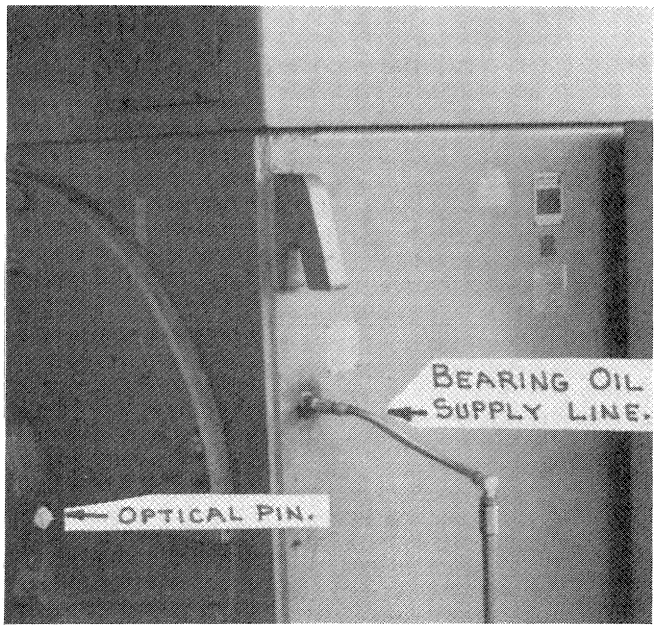

Figure 43. Motor Bearing Oil Supply Is Furnished by Braided Flexible Hose. Note Optical Pin on Bearing Housing.

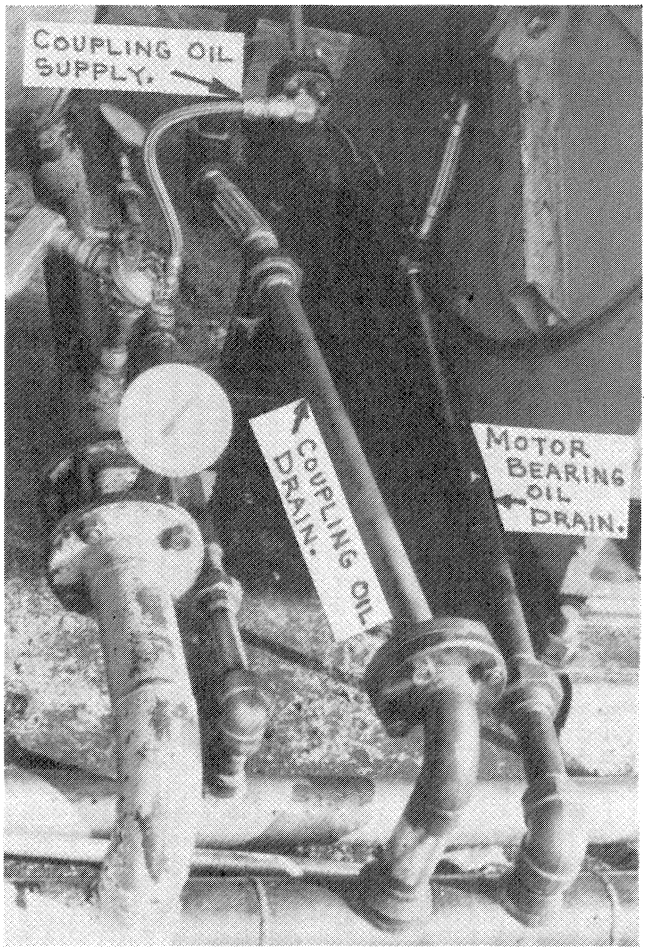

Figure 44. Motor Bearing Oil Return Lines Were Increased in Size from ¾ in. to 1¼ in.

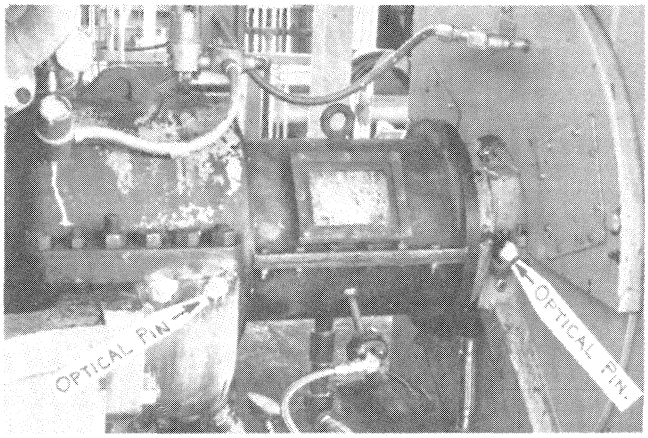

Figure 45. A Coupling Oil Flow Inspection Window Was Installed on the Top Half of Coupling Guard.

Motor Alignment

After the motor was cleaned and the tilting pad bearings installed, it was positioned on the motor soleplates for mechanical alignment. Existing shims from each motor foot had been taped together and identified by location for future use. Shim pack thickness varied from .437 in. to .556 in., with as many as nine shims to the pack. Four steel shim plates were surface ground on both sides to a thickness of 360 in., and one plate was used at each motor foot to reduce the total number of shims. This reduced the possibility of a "soft foot" caused by a spongy shim pack.

Previous data indicated that the compressor had a vertical thermal growth of .008 in. on the inboard end and .001 in. on the outboard. These data were used to plot the desired hot alignment, which determined the cold offset for the motor. The compressor was chosen as the stationary machine because of its size and piping restraints. With an assumed motor vertical thermal growth of .010 in., the motor was aligned high to the compressor by .0225 in. at the inboard feet and .039 in. at the outboard feet. Compressor horizontal thermal growth dictated a cold motor alignment of .005 in. south.

A Houston-based company was contracted to obtain cold and hot optical readings to determine actual hot alignment. Optical bench marks were installed in the concrete foundation for both vertical and horizontal references. Precision dowel pins were installed near the split line of the bearing housings on both compressor and motor (see Figure 45). Each dowel pin location was spot faced with a special cutter that pivoted on the dowel pin. An invar optical scale holder was used to slip over the precision dowel pin and indexed against the spot faced surface of the bearing housing. This provided optical readings that repeated to .001 in. each time the scale holder was removed and replaced. Each optical reading was taken three times before being recorded.

The optical alignment revealed that the compressor had risen .020 in. at the outboard bearing and .042 in. at the inboard bearing. This particular compressor has its discharge nozzle on the inboard end. Since the inboard end of the compressor was the hottest, and the motor cooling air intake was located on the inboard end, the motor raised .025 in. at the inboard bearing and .012 in. at the outboard bearing. No attention had been paid to the location of the motor air intake, but, as illustrated, large thermal growth caused by such an oversight could cause alignment problems. However, in this case, it was not a problem, as illustrated by Figure 46. This alignment plot shows the motor to be .0015 in. high at the compressor coupling hub. An acceptable alignment limit for a coupling of the size used in this installation would be .007 in. Horizontal alignment was also good, with the motor being .001 in. north at the motor coupling hub.

Sometimes a person gets lucky during equipment alignment, but don't count on it. If all assumptions are verified and data accurately recorded, good alignment will result. There are no short cuts in obtaining smooth running equipment.

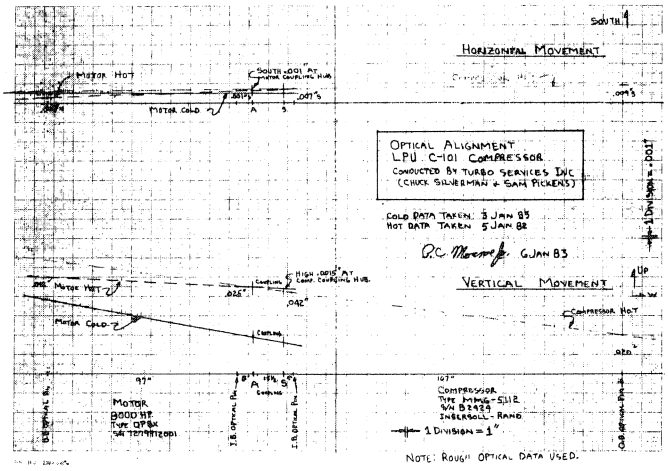

Figure 46. Optical Alignment Plot of Hot Mechanical Alignment.

With the mechanical alignment completed, the power was connected to the motor. To speed up alignment, other crafts were excluded from the compressor deck. Once the electricians had completed their jobs, the motor was ready for a solo run.

Start up

Prior to the motor solo run, all monitoring instrumentation was checked and calibrated. The motor was then run for two hours with the new tilting pad bearings and coupling hub. Vibration amplitudes stabilized within ten minutes of start-up, with a maximum level of 1.0 mil on the outboard horizontal position. The cascade plots of the vertical outboard (Figure 47) and the vertical inboard (Figure 48) vibrations showed no subsynchronous frequencies. All vital signs were normal, so the motor was shut down and the coupling installed. The coupling guard was then installed and the coupling lube oil spray nozzles checked for flow rate and position.

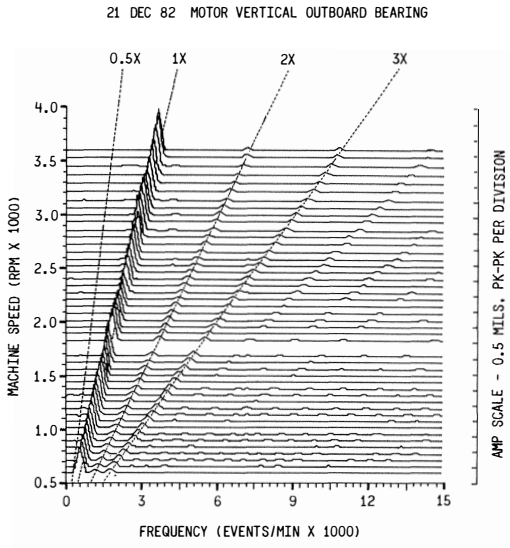

Figure 47. Cascade Plot of the Vertical Outboard Vibration During Solo Run of Motor.

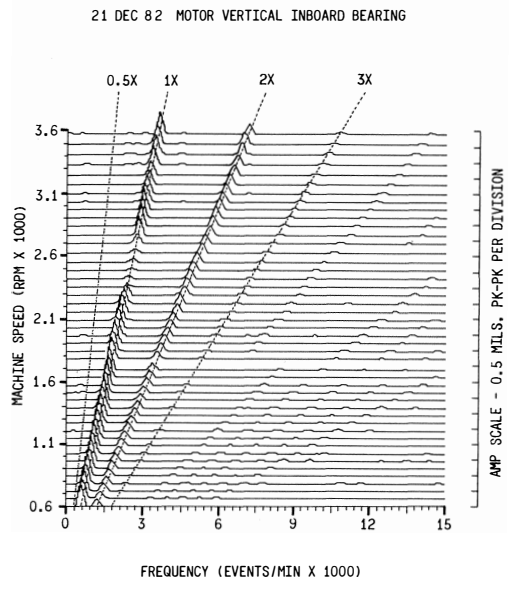

Figure 48. Cascade Plot of the Vertical Inboard Vibration During Solo Run of Motor.

On January 4, 1983, the compressor train was brought on stream. The start-up went very smoothly, and all vibration and temperature levels stabilized in seven hours. A team recorded all vital signs for eight hours. No sub-synchronous frequencies were apparent in the motor, and the maximum vibration was 1.8 mils on the outboard horizontal position. Cascade plots of the vertical outboard (Figure 49) and vertical inboard (Figure 50) vibrations show no sub-synchronous frequencies, even with the compressor loaded. Figures 51 and 52 clearly illustrate that there are no abnormal frequency components at full speed and full load.

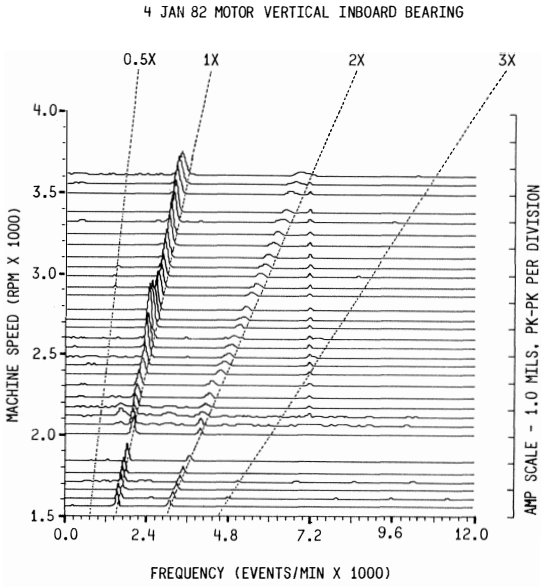

Figure 49. Cascade Plot of the Vertical Outboard Motor Vibration During Compressor Train Start-up. Notice No Sub-Synchronous Frequencies.

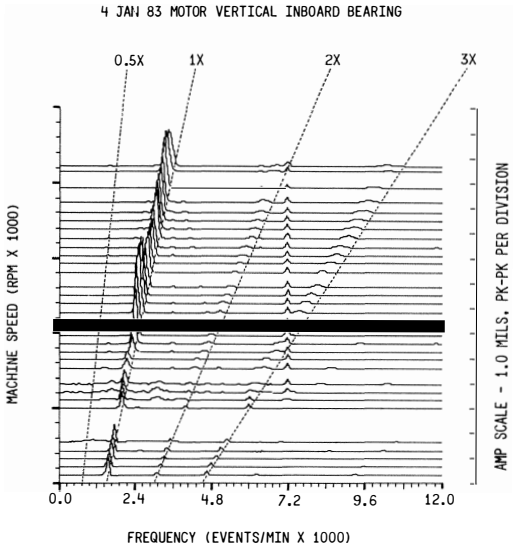

Figure 50. Cascade Plot of Vertical Inboard Motor Vibration During Compressor Train Start-up. Notice No Sub-Synchronous Frequencies.

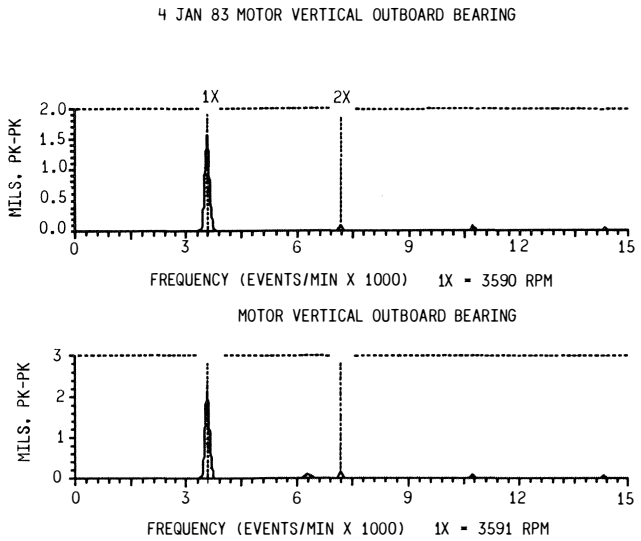

Figure 51. Frequency Analysis of Outboard Motor Bearing Vibration Signals One Hour After Start-up Showed No Sub-Synchronous Frequencies.

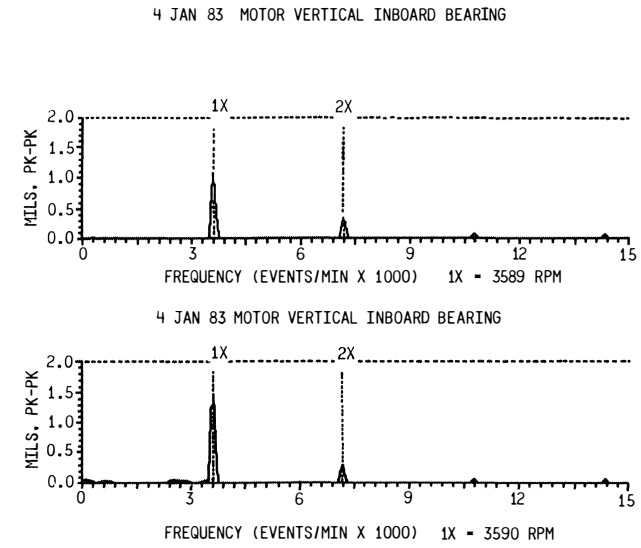

Figure 52. Frequency Analysis of Inboard Motor Bearing Vibration Signals One Hour After Start-up Showed No Sub-Synchronous Frequencies.

On January 6, 1983, additional vibration data were taken after the compressor train had reached a steady state condition. Figure 53 is a typical example of the motor bearing vibration amplitudes and frequencies.

As of the writing of this paper, the tilting pad bearings have functioned flawlessly and converted a once troublesome compressor train into a properly acting piece of turbomachinery.

There are future plans to replace the existing gear coupling with a non-lubricated diaphragm coupling. Computer studies of the proposed couplings indicate a further reduction in vibration levels due to the reduced overhung weight.

CONCLUSIONS

Perhaps the single largest lesson learned from the example in this paper was that two-pole electric motors must be

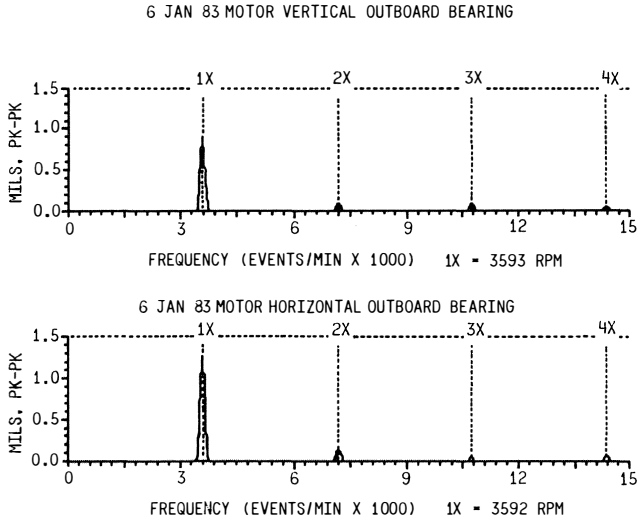

Figure 53. Frequency Analysis of Outboard Motor Bearing Vibration Signals with Compressor Train at Steady State (Two Days After Start-up) Showed No Sub-Synchronous Frequencies.

treated like pieces of turbomachinery. Lessons learned on how to specify and operate turbines and compressors must be applied to 3600 rpm high energy motors. Rotor instability problems in operating two-pole motors that have not received the "Turbomachinery Treatment" can be solved on-stream by use of the computer and other existing techniques.

High energy and high speed turbomachinery trains need continuous vibration and temperature monitoring systems that are armed for shutdown. Computer systems are available that store large amounts of equipment vital signs, which then can be used for shutdown voting logic. These stored data enhance solutions to turbomachinery problems by correlation of operating data prior to, during and after shutdown.

Field observations, suspicions, and desires must be plugged into the analytical solution. This approach can greatly reduce the fields of investigation, as well as verify analytical assumptions and solutions. Both of these points are illustrated by the example in this paper. Solutions to turbomachinery problems are much faster when equipment manufacturers supply dimensional information. Users are not in the business of manufacturing parts, but are charged with making the equipment produce. Users get involved in hardware manufacturing only when their needs are not met swiftly and professionally.

The solution of any turbomachinery problem is directly influenced by the quality of workmanship during installation of hardware. Attention to details, with pictorial and written chronicling of events, is absolutely necessary. Achieving this goal is enhanced by placing a turbomachinery engineer on the deck during repairs.

Wise use of available tools and resources is key to the development of a team effort in turbomachinery problem solving.

REFERENCES

1. Barrett, L. E., Gunter, E. J., and Allaire, P. E., "Optimum Bearing and Support Damping for Unbalance Response and Stability of Rotating Machinery," Journal of Engineering for Power, Trans. ASME, *100*, 1, pp. 89-94 (1978).

2. Lund, J. W. and Orcutt, F. K., "Calculations and Experiments on the Unbalance Response of a Flexible Rotor," Journal of Engineering for Industry, Trans. ASME, Series B, *89*, pp. 785-796 (1967).

3. Salamone, D. J. and Gunter, E. J., "Effects of Shaft Warp and Disk Skew on the Synchronous Unbalance Response of a Multimass Flexible Rotor in Fluid Film Bearings," In *Topics in Fluid Film Bearing and Rotor Bearing System Design and Optimization*, ASME Book No. 100118 (1978).

4. Gunter, E. J., *Dynamic Stability of Rotor-Bearing Systems*, NASA SP-113, Office of Technical Utilization, U.S. Government Printing Office, Washington, D.C. (1966).

5. Lund, J. W., "Stability and Damped Critical Speeds of a Flexible Rotor in Fluid Bearings." Journal of Engineering for Industry, Trans. ASME, Series B, *96*, pp. 509-517 (1974).

ACKNOWLEDGEMENT

Many thanks to Terry Hernandez, Senior Engineer at the Exxon Chemical Baytown Plant, for his relentless pursuit of a phantom vibration problem and his long hours spent installing the new motor bearings. His tenaciousness and attention to detail were major ingredients in the successful solution of this motor problem.